Supplementary Information for
Vibrational infrared and Raman spectra of the methanol molecule with equivariant neural-network property surfaces

Ayaki Sunaga,[1] Albert P. Bartók,[2,3] and Edit Mátyus[1,*]

[1] *ELTE, Eötvös Loránd University, Institute of Chemistry,*
Pázmány Péter sétány 1/A 1117 Budapest, Hungary

[2] *Department of Physics, University of Warwick, Coventry, CV4 7AL, UK*

[3] *Warwick Centre for Predictive Modelling, School of Engineering,*
University of Warwick, Coventry, CV4 7AL, UK

(Dated: April 8, 2026)

CONTENTS

S1. Development process of the property surfaces 2

S2. Convergence test with the number of geometry points in the training set 3

S3. Assignment of the vibrational states and comparison with experiment 6

References 13

---

[*] edit.matyus@ttk.elte.hu

S1. DEVELOPMENT PROCESS OF THE PROPERTY SURFACES

To obtain the training sets for fitting and test sets for evaluating the surfaces' quality, we first carry out the electronic structure computation for the 39 401 geometries in the fitting set obtained in Ref. 1. The property surface of the α_{zz} component was unstable when we performed the fit using all the geometry points. Therefore, we extracted the nine geometries that showed negative eigenvalues during the linear response computation of polarizability; these points corresponded to largely distorted structures, and the $|\alpha_{zz}|$ values exceeded 90 $e^2a_0^2E_\mathrm{h}^{-1}$. In the end, we included 35 000 geometries in the training set, and the remaining 4 392 geometries formed the test set. These geometries were randomly extracted from the total 39 392 geometries, and three randomly extracted sets were tested. The qualities of these surfaces are summarized in Tables S1 and S2. The key input parameters of MACE employed in the fitting are provided in Table 1 of the main text.

Based on comparison of the developed property surfaces, SET1 is employed for the dipole moment surface, and SET3 is employed for the polarizability surface in the computation shown in the main text and in the following sections. However, no significant difference is observed in the RMSE errors of the different SETs. This observation suggests that the results are insensitive to precise manner the geometry points are extracted from the geometry set of 39 401 points. The accuracy of the dipole moment and polarizability surfaces obtained with SET1-3 is sufficient and comparable to that of the quantum-chemical computations.

The dependence of the training results on hyperparameters is provided in Tables S3 and S4. Although slight improvement (*i.e.,* the decrease of the RMSE and MAPE) is observed in the polarizability surface trained with $B = 64$ and $\nu = 4$ compared with those listed in Tables S1 and S2, the parameter dependence is much smaller than the diagonal components at the equilibrium, ca. 20 $e^2a_0^2E_\mathrm{h}^{-1}$ (Table 2 of the main text). For the dipole moment surfaces, the parameters employed in (SET1) are the best choice among the parameters investigated in Tables S1 and S2.

The MACE program[2] at commit hash a8f2f6cd64e7 was used for the fitting of the property surfaces.

TABLE S1. Root mean square error (RMSE) of the polarizability and dipole moment surfaces for methanol in $e^2a_0^2E_\mathrm{h}^{-1}$ for polarizability and ea_0 for dipole moment, fitted by the MACE program. The *ab initio* values are obtained at the CCSD/aug-cc-pVTZ level of theory.

		polarizability						dipole moment		
		xx	yy	zz	xy	yz	xz	x	y	z
SET1	training	0.047	0.053	0.087	0.029	0.048	0.032	0.0018	0.0028	0.0028
	test	0.049	0.056	0.103	0.028	0.048	0.029	0.0018	0.0026	0.0031
SET2	training	0.048	0.054	0.082	0.029	0.046	0.032	0.0020	0.0030	0.0030
	test	0.044	0.048	0.080	0.031	0.044	0.029	0.0018	0.0035	0.0030
SET3	training	0.048	0.052	0.079	0.029	0.046	0.032	0.0019	0.0028	0.0029
	test	0.049	0.057	0.080	0.028	0.046	0.030	0.0017	0.0026	0.0029

TABLE S2. Mean absolute percentage error (MAPE, %) of the polarizability and dipole moment surfaces for methanol, fitted by MACE program. The *ab initio* values are obtained at the CCSD/aug-cc-pVTZ level of theory.

		polarizability						dipole moment		
		xx	yy	zz	xy	yz	xz	x	y	z
SET1	training	0.15	0.16	0.16	21.82	19.97	17.22	42.95	0.41	1.34
	test	0.15	0.16	0.16	53.84	17.50	20.63	20.86	0.40	1.05
SET2	training	0.15	0.16	0.16	20.54	17.12	18.81	54.47	0.42	1.58
	test	0.15	0.16	0.16	41.98	14.52	21.66	24.73	0.48	1.00
SET3	training	0.15	0.16	0.16	27.11	19.06	18.68	26.48	0.41	1.24
	test	0.16	0.16	0.16	19.79	29.20	16.00	175.37	0.42	1.19

TABLE S3. Root mean square error (RMSE) of the polarizability, in $e^2a_0^2E_\mathrm{h}^{-1}$, and dipole moment, in ea_0, fitted with the MACE program using various hyperparameters. B: batch size, ν: correlation order. All other parameters are the same as in Table 1 of the main text. The *ab initio* values are obtained at the CCSD/aug-cc-pVTZ level of theory.

		xx	yy	zz	xy	yz	xz	x	y	z
$B = 64$	training	0.055	0.060	0.087	0.033	0.033	0.037	0.0024	0.0035	0.0034
	test	0.055	0.064	0.084	0.031	0.031	0.032	0.0023	0.0033	0.0036
$B = 16$	training	0.044	0.048	0.075	0.027	0.027	0.029	0.0021	0.0029	0.0029
	test	0.044	0.052	0.077	0.027	0.027	0.028	0.0021	0.0028	0.0030
$\nu = 4$	training	0.039	0.046	0.067	0.025	0.025	0.030	0.0020	0.0029	0.0028
	test	0.046	0.055	0.063	0.024	0.024	0.027	0.0019	0.0028	0.0028

TABLE S4. Mean absolute percentage error (MAPE, %) of the polarizability and dipole moment surfaces for methanol, fitted with the MACE program using various hyperparameters. B: batch size, ν: correlation order. All other parameters are the same as in Table 1 of the main text. The *ab initio* values are obtained at the CCSD/aug-cc-pVTZ level of theory.

		xx	yy	zz	xy	yz	xz	x	y	z
$B = 64$	training	0.18	0.18	0.17	28.40	28.40	21.01	91.97	0.52	1.58
	test	0.18	0.18	0.17	20.63	20.63	20.92	30.62	0.54	1.06
$B = 16$	training	0.14	0.14	0.15	19.26	19.26	16.59	72.35	0.44	1.34
	test	0.14	0.15	0.15	19.14	19.14	19.03	26.59	0.46	0.91
$\nu = 4$	training	0.12	0.14	0.14	22.62	22.62	18.00	73.14	0.43	1.31
	test	0.13	0.15	0.14	26.36	26.36	17.35	23.80	0.43	0.95

S2. CONVERGENCE TEST WITH THE NUMBER OF GEOMETRY POINTS IN THE TRAINING SET

The convergence with respect to the number of geometry points was investigated using SET1 for dipole moment and SET3 for polarizability. We designed the training set with fewer geometries to be a subset of the training set with more geometries. For example, the training set with 30 000 geometries (geometries in the test set) was obtained by randomly extracting 5 000 geometries from the 35 000 geometries in the training set and moving them to the test set (FIGs. S1 and S2).

The RMSE basically decreases as the number of geometry points in the training set increases. The error is not monotonically decreasing due to largely distorted geometries, picked randomly in the training/test sets. Most components are converged with respect to the number of geometries, but the RMSE of the off-diagonal components of α_{ij} could be decreased further. However, since the RMSE errors of the off-diagonal part are sufficiently smaller than the diagonal errors, we do not have to increase the number of geometries. We should note that the components with large values (the y and z components of μ and the diagonal components of α_{ij}) are converged with a smaller number of geometry points: approximately 20 000 geometries (5000 geometries) are sufficient to achieve the error below 2% (1%) of the μ (α_{ii}). The components with small values (the x component of μ and the off-diagonal components of α_{ij}) show relatively large MAPEs because some of their values are close to zero.

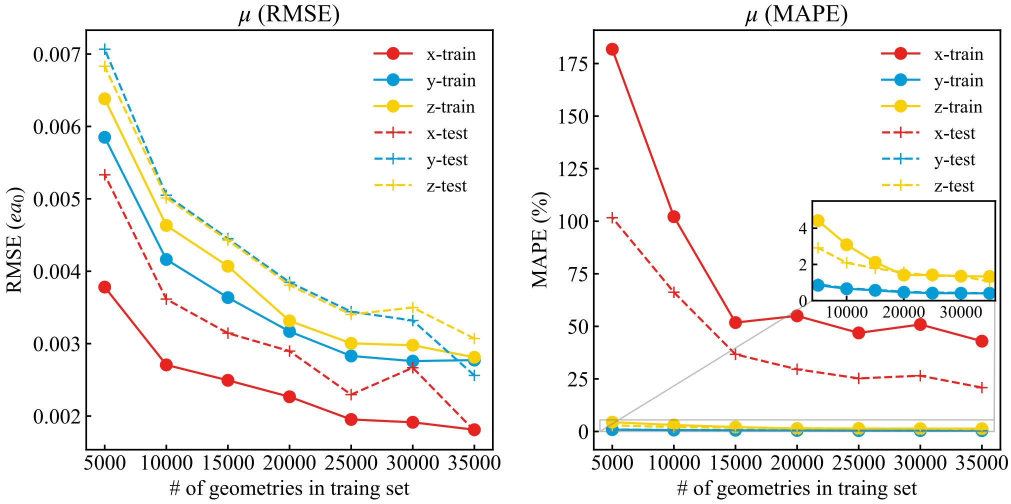

FIG. S1. RMSE in ea_0 and MAPE in % for the training set and test set obtained with dipole moment surface of the methanol molecule. The data points were computed at the CCSD/aug-cc-pVTZ level of theory.

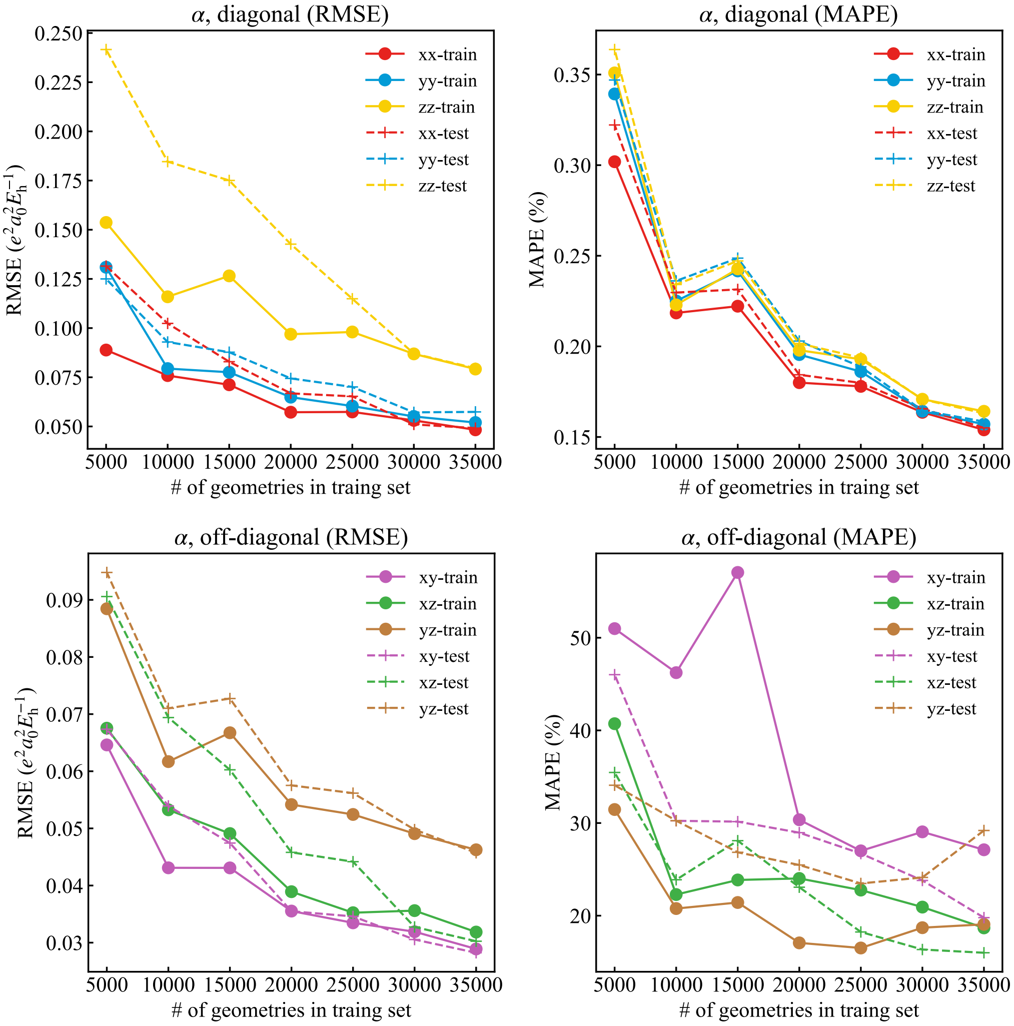

FIG. S2. RMSE in $e^2a_0^2E_\mathrm{h}^{-1}$ and MAPE in % for the training set and test set obtained with polarizability surface for the methanol molecule. The data points were computed at the CCSD/aug-cc-pVTZ level of theory.

S3. ASSIGNMENT OF THE VIBRATIONAL STATES AND COMPARISON WITH EXPERIMENT

In Tables S6-S11, we list the vibrational states up to the OH stretching fundamental vibrational as obtained with the GENIUSH-Smolyak method ($b = 7$ vibrational basis[3] and PES2025[1]) and available data originating from gas-phase experiment. The first 150 vibrational states were already listed in the Tables S7–S9 of Ref. 1. We extend it with the further 525 states obtained since the publication of that paper. Table S5 lists the harmonic frequencies of PES2025[1] and corresponding labels, which allows us to define the vibrational labels used to assign the variational vibrational states.

The vibrational energies of the fundamental modes are listed in Table 3 of the main text, but we note that strong torsion-vibration mixing is observed for ν_6 (No. 25-27), whereas mode coupling is observed for ν_7 (No. 17-19), ν_3 (No. 265, 268-269), and ν_2 (No. 311-313). The importance of coupling of 3_1 and 5_2 (No. 265), and 9_1 and $4_1 + 10_1$ (No. 313) was already pointed out in a vibrational configurational interaction computation (Table S3 of Ref. 4). The coupling between the torsional and CH stretch motion was also investigated in Refs. 5 and 6.

TABLE S5. Harmonic frequencies corresponding to PES2025[1] used in this work. Γ is the symmetry label (deliberately in small letters referring to 'single mode') corresponding to the $C_{3\mathrm{v}}$(M) molecular symmetry group.

Label	Description	coord	Γ	$\tilde{\nu}$ [cm^{-1}]
ν_1	ν(OH)	r_{OH}	a_1	3864.31
ν_2	$\nu(\mathrm{CH}_3)_{\mathrm{asym}}$	r_{CH}	e	3099.06
ν_9	$\nu(\mathrm{CH}_3)_{\mathrm{asym}}$	r_{CH}	e	3099.06
ν_3	$\nu(\mathrm{CH}_3)_{\mathrm{sym}}$	r_{CH}	a_1	3024.56
ν_4	$\delta(\mathrm{CH}_3)_{\mathrm{asym}}$	φ_2	e	1517.64
ν_{10}	$\delta(\mathrm{CH}_3)_{\mathrm{asym}}$	φ_1	e	1517.64
ν_5	$\delta(\mathrm{CH}_3)_{\mathrm{sym}}$	θ_{HCO}	a_1	1486.35
ν_6	δ(COH)	θ_{COH}	a_1	1280.06
ν_{11}	$\rho(\mathrm{CH}_3)$	θ_{HCO}	e	1183.72
ν_7	$\rho(\mathrm{CH}_3)$	θ_{HCO}	e	1183.72
ν_8	ν(CO)	r_{CO}	a_1	1076.05

TABLE S6. Vibrational energies, $\tilde{\nu}_{\mathrm{PES}}$ in cm^{-1}, referenced to the zero-point vibrational energy (ZPVE, 11119.58 cm^{-1}) of CH_3OH in 12D computed with the GENIUSH-Smolyak program with the $b = 7$ basis set and using PES2025.[1] The first 150 vibrational states are listed in Tables S7-S9 of the Supplementary Material of Ref. 1. Comparison with the vibrational band origins derived from (gas-phase) experiment is shown as $\delta = \tilde{\nu}_{\mathrm{exp}} - \tilde{\nu}_{\mathrm{PES}}$, in cm^{-1}. SAMs: assignment of the curvilinear normal modes $1_n, 2_n, \ldots, 11_n (n = 0, 1, \ldots)$ (Table S5), no excitation ($n = 0$) is noted as "0". "[...]" labels the largest contribution(s) from strongly mixed states. Γ : $C_{3\mathrm{v}}$(M) label according to Table S5 and the irreducible representations of the torsional part. Further details are in Sec. S1 of the Supporting Information of Ref. 3. All degeneracies for the E states are converged better than 0.01 cm^{-1}, except for the pairs listed in the footnotes.

#	ν_τ	SAMs	Γ	$\tilde{\nu}_{\mathrm{PES}}$	#	ν_τ	SAMs	Γ	$\tilde{\nu}_{\mathrm{PES}}$
151-152	0,2	$[11_1+7_1, 6_1+7_1]$	E	2494.3	208	1	6_2	A_2	2676.0
153-154	4	$[4_1, 10_1]$	E	2497.5	209-210	1	5_1+8_1	E	2690.5
155	3	5_1	A_2	2497.9	211-212	2	$7_1+8_1, 11_1+8_1$	E	2694.2
156	4	5_1	A_1	2498.7	213-214	2	$[7_2, 6_1+7_1]$	E	2695.7
157-158	0	$4_1+8_1, 10_1+8_1$	E	2505.1	215	1	$10_1+8_1, 4_1+8_1$	A_2	2706.2
159-160	2	$7_1+8_1, 11_1+8_1$	E	2506.7	216	1	$4_1+8_1, 10_1+8_1$	A_1	2715.7
161	0	$4_1+8_1, 10_1+8_1$	A_2	2510.5	217-218	1	$[4_1+8_1, 10_1+8_1]$	E	2717.8
162-163	0	$4_1+8_1, 10_1+8_1$	E	2513.6	219	2	6_2	A_1	2726.4
164	0	$10_1+8_1, 4_1+8_1$	A_1	2516.9	220-221	1,2	$[6_2, 11_1+7_1]$	E	2727.9
165	0	$[5_1+6_1, 5_1+11_1]$	A_1	2520.1	222-223	6	0	E	2733.6
166-167	0	$[5_1+11_1, 5_1+6_1]$	E	2523.5	224-225	0	5_1+6_1	E	2744.5
168-169	3,4	$4_1, 10_1$	E	2532.1	226	2	$[7_1+8_1, 11_1+8_1]$	A_2	2745.0
170-171	0	$[10_1+7_1, 10_1+6_1]$	E	2542.5	227	2	$[6_1+11_1, 6_1+7_1]$	A_1	2759.9
172	0	$[10_1+7_1, 4_1+11_1]$	A_2	2545.4	228	1	$[5_1+8_1, 5_1+11_1]$	A_2	2760.8
173-174	0	$[7_2, 4_1+7_1]$	E	2548.0	229	0,1	$[5_1+6_1, 5_1+11_1]$	A_1	2764.8
175	0	$[4_1+7_1, 10_1+11_1]$	A_1	2553.0	230-231	0	$[10_1+6_1, 4_1+6_1]$	E	2765.8
176-177	1	$[11_1+7_1, 11_2]$	E	2554.0	232	0	$4_1+6_1, 10_1+6_1$	A_1	2767.2
178	2	$[6_1+8_1, 7_1+8_1]$	A_1	2562.5	233	1	5_1+8_1	A_2	2769.3
179-180	4	$11_1, 7_1$	E[a]	2566.2	234-235	2	6_1+8_1	E	2773.8
181	4	$11_1, 7_1$	A_2	2567.6	236	2	$[6_1+8_1, 11_1+8_1]$	A_1	2776.5
182	1	6_1+8_1	A_2	2571.3	237	1	$[6_1+7_1, 6_1+11_1]$	A_2	2779.7
183-184	2	8_2	E	2574.3	238-239	0,1	$[4_1+6_1, 4_1+7_1]$	E	2780.8
185	4	$11_1, 7_1$	A_1	2575.4	240-241	1	$10_1+8_1, 5_1+6_1$	E	2788.9
186	4	$[7_1, 11_1]$	A_2	2585.9	242	1	5_1+8_1	A_2	2790.5
187	2	6_1+8_1	A_1	2588.7	243-244	1	$[4_1+11_1, 5_1+6_1]$	E	2793.9
188-189	1,2	$[6_2, 6_1+7_1]$	E	2589.9	245-246	3	8_2	E	2800.7
190-191	0	5_1+7_1	E	2597.5	247	1	$10_1+6_1, 4_1+6_1$	A_2	2806.5
192	0	$5_1+7_1, 5_1+11_1$	A_2	2603.0	248	1	$4_1+6_1, 10_1+6_1$	A_1	2809.4
193-194	1	6_1+8_1	E	2606.1	249-250	1	$[4_1+8_1, 10_1+6_1]$	E	2810.3
195-196	1,2	11_1+7_1	E	2616.1	251-252	1	$4_1+8_1, 10_1+8_1$	E	2812.3
197	0	$10_1+11_1, 4_1+7_1$	A_1	2618.6	253	0	$[5_1+11_1, 5_1+7_1]$	A_1	2816.2
198-199	0	$4_1+7_1, 10_1+11_1$	E	2621.5	254	2	11_1+7_1	A_2	2816.8
200	0	$[10_1+7_1, 4_1+11_1]$	A_2	2624.3	255	2	11_1+7_1	A_1	2817.8
201-202	0	$4_1+11_1, 10_1+7_1$	E	2629.9	256-257	0,2	$[11_1+7_1, 6_2]$	E	2819.1
203-204	0,2	$[6_2, 6_1+11_1]$	E	2650.0	258-259	0	$[10_1+11_1, 10_1+7_1]$	E	2836.3
205-206	4	6_1	E	2667.3	260	2	5_1+8_1	A_1	2836.8
207	0	$[6_2, 6_1+11_1]$	A_1	2669.9					

[a] 2566.163,2566.179

TABLE S7. Vibrational states of CH_3OH... [Table S6 continued]

#	ν_τ	SAMs	Γ	$\tilde{\nu}_{\text{PES}}$	δ	$\tilde{\nu}_{\text{exp}}$	
261-262	5	8_1	E	2837.3			
263-264	4	$4_1, 10_1$	E	2841.7			
265	0	$3_1, 5_2$	A_1	2841.8	[3.0]	[a]2844.7	5
266-267	4	5_1	E	2845.1			
268-269	0	$[3_1, 5_2]$	E	2850.7	[3.1]	[a]2853.8	5
270-271	2	$4_1 + 8_1$	E	2862.0			
272-273	2	$[7_2, 11_2]$	E	2867.8			
274-275	1	$5_1 + 7_1, 5_1 + 11_1$	E	2870.7			
276	4	$10_1, 4_1$	A_2	2878.6			
277	4	$4_1, 10_1$	A_1	2879.6			
278-279	1	$4_1 + 11_1, 10_1 + 7_1$	E	2888.7			
280	1	$[4_1 + 7_1, 10_1 + 11_1]$	A_2	2891.9			
281	1	$[10_1 + 7_1, 4_1 + 11_1]$	A_1	2892.9	[0.3]	[b]2893.2	7
282-283	2	$[6_1 + 7_1, 6_1 + 11_1]$	E	2900.4			
284-285	0	$4_1 + 5_1, 10_1 + 5_1$	E	2913.2	[–3]	[c]2910	7
286	0	$[4_1 + 5_1, 10_1 + 5_1]$	A_2	2917.8	[–6]	2912	7
287	0	5_2	A_1	2920.9			
288-289	0,2	$[10_1 + 5_1, 5_1 + 11_1]$	E	2921.5			
290-291	2	$5_1 + 7_1, 5_1 + 11_1$	E	2923.1			
292	0	$[4_1 + 5_1, 4_1 + 10_1]$	A_1	2928.4	[1.1]	2929.5	7
293-294	0	$[10_1 + 5_1, 2_1]$	E	2930.3			
295-296	0	$5_2, 4_2$	E	2931.6			
297	0	$4_1 + 5_1, 10_1 + 5_1$	A_2	2933.9			
298-299	2	$[4_1 + 11_1, 10_1 + 7_1]$	E	2934.1			
300	3	$7_1 + 8_1, 11_1 + 8_1$	A_1	2935.1			
301	3	$7_1 + 8_1, 11_1 + 8_1$	A_2	2935.3			
302-303	0	$[4_1 + 10_1, 4_2]$	E	2938.5			
304	0	$4_1 + 10_1$	A_1	2939.2			
305	1	6_2	A_2	2940.3			
306-307	1,2	$[6_1 + 7_1, 11_1 + 7_1]$	E	2948.1			
308	2	$4_1 + 7_1, 10_1 + 11_1$	A_1	2952.2			
309	2	$10_1 + 7_1, 4_1 + 11_1$	A_2	2956.1			
310	0	$[4_2, 10_2]$	A_1	2957.0	[1.4]	[a]2958.4	5
311-312	0	$[4_1 + 10_1, 2_1, 9_1]$	E	2959.1	[2.1]	2961.2	8
313	0	$[4_1 + 10_1, 2_1, 9_1]$	A_2	2964.2	[2.5]	2966.7	8
314-315	0	$[4_2, 10_2]$	E	2964.7	[2.0]	[a]2966.7	5
316-317	5	$7_1, 11_1$	E	2965.0			
318	2	6_2	A_1	2966.6			
319	5	$7_1, 11_1$	A_2	2974.3			
320	5	$11_1, 7_1$	A_1	2974.3			
321-322	2	$[6_2, 6_1 + 7_1]$	E	2975.3			
323-324	3	$[7_1 + 8_1, 11_1 + 8_1]$	E	2989.0			
325	1	$5_1 + 6_1$	A_2	2989.3			
326-327	2	$5_1 + 8_1$	E	2994.7			
328	2	$5_1 + 6_1$	A_1	2995.1			
329-330	0	$[2_1, 9_1]$	E	2999.8	[3.9]	3003.7	9
331	0	$9_1, 2_1$	A_1	3002.9	[4.1]	3007.0	9

[a] The values listed in Table I of Ref. 5 are shifted by the zero-point energy of 128.1 cm^{-1}, taken from in Ref. 8.

[b] The assignment of Ref. 7 is 5_2.

[c] The assignment of Ref. 7 is 10_2.

TABLE S8. Vibrational states of CH_3OH… [Table S7 continued]

#	ν_τ	SAMs	Γ	$\tilde{\nu}_{\mathrm{PES}}$	#	ν_τ	SAMs	Γ	$\tilde{\nu}_{\mathrm{PES}}$
332-333	1	$4_1+6_1, 10_1+6_1$	E	3003.8	382	3,2	$[11_1+7_1, 6_1+11_1]$	A_1	3157.4
334-335	2	$4_1+8_1, 10_1+8_1$	E	3006.6	383-384	1	$[4_2, 3_1]$	E	3158.9
336-337	2	$[4_1+6_1, 4_1+11_1]$	E	3019.0	385	3	$6_1+7_1, 6_1+11_1$	A_2	3159.3
338-339	1	$[5_1+6_1, 5_1+6_1]$	E	3021.2	386	3	$6_1+11_1, 6_1+7_1$	A_1	3160.9
340-341	3	6_1+8_1	E	3025.6	387	2	$[5_1+11_1, 5_1+7_1]$	A_2	3162.4
342	2	$4_1+8_1, 10_1+8_1$	A_2	3028.2	388	0	$[6_1+7_1+8_1, 6_1+11_1+8_1]$	A_1	3168.8
343	2	$10_1+8_1, 4_1+8_1$	A_1	3030.4	389-390	0	$[7_1+8_2, 6_1+7_1+8_1]$	E	3170.8
344	1	$[10_1+6_1, 4_1+6_1]$	A_2	3034.3	391	1	$[4_1+10_1, 9_1]$	A_1	3175.8
345	1	$[10_1+6_1, 4_1+6_1]$	A_1	3040.2	392-393	1,2	$[4_1+11_1, 4_1+10_1]$	E	3176.7
346-347	1	$[4_1+6_1, 10_1+6_1]$	E	3042.1	394-395	2	$[4_1+7_1, 4_1+11_1]$	E	3179.2
348-349	1	$3_1, 5_2$	E	3056.5	396	2	$[5_1+6_1, 5_1+11_1]$	A_1	3187.6
350-351	3	11_1+7_1	E	3071.5	397	1	$2_1, 9_1$	A_2	3190.4
352	0	8_3	A_1	3077.7	398-399	2	5_1+6_1	E	3191.4
353-354	5	6_1	E	3084.7	400-401	2	6_2	E	3192.6
355-356	0	8_3	E	3086.4	402-403	2	$4_1+6_1, 10_1+6_1$	E	3195.1
357-358	3	$7_2, 11_2$	E	3102.0	404	2	$3_1, 5_2$	A_1	3201.4
359	3	8_2	A_2	3102.2	405-406	0	$7_1+8_2, 11_1+8_2$	E	3202.2
360	4	8_2	A_1	3103.2	407	0	$7_1+8_2, 11_1+8_2$	A_2	3210.1
361-362	2	$5_1+7_1, 5_1+11_1$	E	3107.5	408-409	2	$[4_1+6_1, 4_1+7_1]$	E	3210.4
363	2	$[10_1+11_1, 4_1+7_1]$	A_2	3109.0	410-411	1	4_1+5_1	E	3211.8
364	2	$[4_1+7_1, 10_1+7_1]$	A_1	3110.7	412	0	$[6_1+7_2, 6_1+11_2]$	A_1	3214.1
365	1	$10_1+5_1, 4_1+5_1$	A_2	3121.2	413-414	0	$[6_1+7_2, 6_2+7_1]$	E	3215.2
366	0	$[8_3, 6_1+8_2]$	A_1	3123.5	415	1	5_2	A_2	3215.9
367-368	1	$[4_2, 4_1+10_1]$	E	3124.0	416	2	$4_1+6_1, 10_1+6_1$	A_1	3223.6
369	1	$10_1+5_1, 4_1+5_1$	A_1	3127.4	417-418	1	$[4_1+10_1, 4_2]$	E	3223.6
370-371	0	$[8_3, 7_1+8_2]$	E	3127.9	419	2	$4_1+6_1, 10_1+6_1$	A_2	3224.6
372	1	3_1	A_2	3130.6	420-421	3	5_1+8_1	E	3225.5
373-374	1	$[4_1+5_1, 10_1+5_1]$	E	3133.4	422	5	$[4_1, 10_1]$	A_2	3228.2
375-376	1	$[4_2, 5_2]$	E	3137.6	423	5	$[4_1, 10_1]$	A_1	3228.3
377	1	$[4_1+10_1, 10_1+5_1]$	A_1	3141.3	424-425	3,4	$7_1+8_1, 11_1+8_1$	E	3238.0
378-379	2	$[4_1+11_1, 10_1+7_1]$	E	3143.4	426-427	3	6_2	E	3238.7
380	1,3	$[4_1+10_1, 11_1+7_1]$	A_2	3146.7	428-429	5	5_1	E	3247.1
381	3,2	$[11_1+7_1, 6_1+11_1]$	A_2	3151.9	430-431	0	$[11_1+7_1+8_1, 6_1+7_1+8_1]$	E	3247.5

TABLE S9. Vibrational states of CH_3OH... [Table S8 continued]

#	ν_τ	SAMs	Γ	$\tilde{\nu}_{\mathrm{PES}}$	#	ν_τ	SAMs	Γ	$\tilde{\nu}_{\mathrm{PES}}$
432	1	$[3_1, 10_2]$	A_2	3248.6	483	3	$11_2, 7_2$	A_2	3391.0
433	3	$[4_1 + 8_1, 10_1 + 8_1]$	A_1	3252.2	484	4	$7_2, 11_2$	A_1	3391.8
434	3	$[4_1 + 8_1, 10_1 + 8_1]$	A_2	3252.2	485-486	3	$[10_1 + 11_1, 4_1 + 7_1]$	E	3393.8
435	0,1	$[7_1 + 8_1, 11_1 + 7_1 + 8_1]$	A_2	3256.7	487	1	8_3	A_2	3393.9
436-437	3,4	$[7_1 + 8_1, 11_1 + 8_1]$	E[a]	3262.2	488-489	3	$[5_1 + 7_1, 5_1 + 11_1]$	E	3397.9
438-439	3	$[4_1 + 8_1, 10_1 + 8_1]$	E[b]	3262.5	490	0,1	$[6_2 + 8_1, 11_1 + 8_2]$	A_1	3403.7
440-441	1	$2_1, 9_1$	E	3264.6	491-492	3	$[4_1 + 11_1, 10_1 + 7_1]$	E[f]	3405.6
442-443	2	$4_1 + 5_1, 10_1 + 5_1$	E[c]	3273.3	493-494	0,1	$[6_2 + 8_1, 7_2 + 8_1]$	E	3411.8
444-445	7	0	E[d]	3273.8	495	2	$4_1 + 10_1$	A_2	3413.1
446	5	8_1	A_2	3276.3	496	2	$4_1 + 10_1$	A_1	3415.3
447	6	8_1	A_1	3276.3	497	0	$[6_1 + 8_2, 7_1 + 8_2]$	A_1	3417.4
448	2	5_2	A_1	3278.9	498-499	2	$10_1 + 5_1, 4_1 + 5_1$	E	3417.9
449-450	1	8_3	E	3286.0	500-501	5,6	$7_1, 11_1$	E[g]	3422.8
451-452	2	$4_1 + 10_1$	E	3287.4	502-503	3,4	$11_1 + 7_1$	E[h]	3425.2
453-454	5	$10_1, 4_1$	E[e]	3290.9	504	3	$[4_1 + 11_1, 10_1 + 11_1]$	A_2	3425.5
455-456	0	$6_1 + 11_1 + 7_1, 11_2 + 7_1$	E	3293.5	505	3	$[10_1 + 11_1, 4_1 + 11_1]$	A_1	3425.9
457	0	$[11_2 + 7_1, 6_1 + 11_1 + 7_1]$	A_2	3301.9	506	0	$[6_1 + 7_1 + 8_1, 6_1 + 11_1 + 8_1]$	A_2	3427.4
458	2	$[3_1, 4_2]$	A_1	3307.6	507-508	5,6	$[7_1, 11_1]$	E	3428.6
459	0	$[11_1 + 7_1 + 8_1, 11_2 + 8_1]$	A_1	3323.4	509-510	1	$[6_2 + 8_1, 6_1 + 8_2]$	E	3431.7
460-461	2	$2_1, 9_1$	E	3325.1	511-521	2	$[5_2]$	E	3433.5
462-463	0	$[7_2 + 8_1, 11_2 + 8_1]$	E	3328.9	513	2	8_3	A_1	3435.0
464	3	$6_1 + 8_1$	A_2	3334.0	514-515	3	$5_1 + 6_1$	E	3438.5
465	4	$6_1 + 8_1$	A_1	3334.2	516	2	$4_1 + 5_1, 10_1 + 5_1$	A_2	3439.9
466-467	0	$6_1 + 8_2$	E	3345.9	517	2	$10_1 + 5_1, 4_1 + 5_1$	A_1	3441.6
468-469	2	$[3_1, 5_2]$	E	3352.6	518-519	4	8_2	E	3447.1
470	3	$5_1 + 7_1, 5_1 + 11_1$	A_1	3353.7	520-521	0	$[11_2 + 7_1, 7_3]$	E	3449.5
471	3	$5_1 + 7_1, 5_1 + 11_1$	A_2	3353.7	522	0	$[11_3, 7_3]$	A_2	3450.1
472-473	2	$3_1, 5_2$	E	3356.2	523	3	$10_1 + 6_1, 4_1 + 6_1$	A_2	3452.3
474	0,1	$[6_1 + 8_2, 11_1 + 8_2]$	A_1	3358.1	524	3	$10_1 + 6_1, 4_1 + 6_1$	A_1	3452.7
475	1	8_3	A_2	3359.6	525	0	$[6_3, 6_2 + 11_1]$	A_1	3454.4
476	0	$11_1 + 7_2$	A_1	3367.0	526-527	3	$5_1 + 6_1$	E	3456.3
477-478	3,4	$11_1 + 7_1$	E	3375.3	528-529	2	$3_1, 10_2$	E	3462.9
479-480	3,4	$[11_1 + 7_1, 7_2]$	E	3381.7	530-531	0	$[7_3, 6_3]$	E	3463.5
481-482	1	$6_1 + 8_2$	E	3386.4					

[a] 3262.157, 3262.172
[b] 3262.459, 3262.476
[c] 3273.340, 3273.368
[d] 3273.796, 3273.809
[e] 3290.923, 3290.960
[f] 3405.636, 3405.649
[g] 3422.825, 3422.884
[h] 3425.241, 3425.260

TABLE S10. Vibrational states of CH_3OH. . . [Table S9 continued]

#	ν_τ	SAMs	Γ	$\tilde{\nu}_{\mathrm{PES}}$	#	ν_τ	SAMs	Γ	$\tilde{\nu}_{\mathrm{PES}}$
532-533	1	$[7_1+8_2, 11_1+7_1+8_1]$	E	3471.8	581-582	0	$[4_1+11_1+8_1, 4_1+8_2]$	E	3570.4
534	2	$2_1, 9_1$	A_2	3472.3	583-584	1	$[7_2+8_1, 11_2+8_1]$	E	3571.9
535-536	3,4	$6_1+11_1, 6_1+7_1$	E	3474.3	585	0	$[10_1+8_2, 4_1+8_2]$	A_2	3573.4
537	2	$2_1, 9_1$	A_1	3476.8	586-587	1	$[11_2+7_1, 7_3]$	E	3575.2
538	2	$[2_1, 9_1]$	A_1	3478.3	588	0,2	$[6_1+8_2, 6_2+8_1]$	A_1	3577.9
539-540	0,1	$[6_1+7_1+8_1, 11_1+8_2]$	E	3480.5	589-590	0,1	$[4_1+7_1+8_1, 11_2+7_1]$	E	3578.9
541-542	3	$10_1+6_1, 4_1+6_1$	E[a]	3481.3	591	0	$[10_1+8_2, 4_1+8_2]$	A_1	3580.6
543-544	3	$[6_2, 6_1+11_1]$	E	3490.0	592	0	$[5_1+6_1+7_1, 5_1+6_1+11_1]$	A_1	3586.3
545-546	2	$[4_1+10_1, 2_1]$	E	3492.4	593-594	0	$[5_1+6_1+11_1, 5_1+7_2]$	E	3587.6
547-548	3,4	$[6_2, 6_1+7_1]$	E	3493.2	595	1	6_1+8_2	A_2	3590.7
549	1	$[11_3, 7_3]$	A_2	3495.0	596-597	4	$7_1+8_1, 11_1+8_1$	E[b]	3592.2
550	0	5_1+8_2	A_1	3499.9	598-599	3	$3_1, 5_2$	E	3594.2
551	1	$[6_1+7_1+8_1, 6_1+11_1+8_1]$	A_2	3502.7	600	4	$[7_1+8_1, 11_1+8_1]$	A_2	3594.4
552-553	0	$[5_1+8_2, 5_1+8_2]$	E	3508.2	601-602	2	8_3	E	3596.3
554-555	0,2	$[11_1+7_1+8_1, 6_1+7_1+8_1]$	E	3517.3	603	4	$11_1+8_1, 7_1+8_1$	A_1	3601.4
556-557	0,2	$[7_1+8_2, 11_1+8_2]$	E	3522.4	604-605	1	$[11_1+7_2, 11_3]$	E	3603.2
558	3	5_1+8_1	A_2	3526.3	606	4	$[11_1+8_1, 7_1+8_1]$	A_1	3605.7
559	4	5_1+8_1	A_1	3527.1	607-608	1,2	$[7_1+8_2, 11_1+7_1+8_1]$	E	3608.0
560-561	0	$4_1+8_2, 10_1+8_2$	E	3527.9	609-610	0	$[10_1+6_1+7_1, 10_1+7_2]$	E	3610.4
562-563	1,2	$[7_1+8_2, 11_1+8_2]$	E	3530.2	611	4	$7_1+8_1, 11_1+8_1$	A_2	3611.4
564-565	3,4	$4_1+8_1, 10_1+8_1$	E	3533.4	612	0	$[4_1+6_1+11_1, 10_1+6_1+7_1]$	A_2	3612.1
566	0	$10_1+8_2, 4_1+8_2$	A_2	3535.5	613	2	6_1+8_2	A_1	3616.2
567	1	$[6_2+11_1, 6_2+7_1]$	A_1	3536.2	614-615	0	$[10_1+6_1+11_1, 10_1+11_2]$	E	3619.0
568-569	0	$4_1+8_2, 10_1+8_2$	E	3537.9	616	0	$[10_1+6_1+11_1, 4_1+6_1+7_1]$	A_1	3621.0
570	0	$10_1+8_2, 4_1+8_2$	A_1	3541.0	617-618	0	$[5_1+11_1+8_1, 5_1+7_1+8_1]$	E	3621.2
571	0	$[5_1+6_1+8_1, 5_1+7_1+8_1]$	A_1	3544.5	619	0	$5_1+11_1+8_1, 5_1+7_1+8_1$	A_2	3627.4
572	0,1	$[11_2+7_1, 6_2+7_1]$	A_2	3545.3	620-621	1	6_1+8_2	E	3628.2
573	5	6_1	A_2	3547.6	622-623	0,2	$[11_1+7_1+8_1, 11_3]$	E	3630.0
574	6	6_1	A_1	3547.7	624-625	1,2	$[7_2+8_1, 11_1+7_1+8_1]$	E	3639.5
575-576	0	$[5_1+7_1+8_1, 5_1+8_2]$	E	3548.1	626	0	$4_1+7_1+8_1, 10_1+11_1+8_1$	A_1	3646.3
577	4	6_2	A_1	3561.9	627-628	0	$[4_1+7_1+8_1, 10_1+11_1+8_1]$	E	3649.1
578	3	6_2	A_2	3562.5	629	0	$[4_1+11_1+8_1, 10_1+7_1+8_1]$	E	3650.7
579-580	3,4	$4_1+8_1, 10_1+8_1$	E	3565.4	630-631	3	$[4_1+11_1, 10_1+7_1]$	E	3650.9

[a] 3481.281, 3481.294

[b] 3592.206, 3592.218

TABLE S11. Vibrational states of CH_3OH… [Table S10 continued]

#	ν_τ	SAMs	Γ	$\tilde{\nu}_{\mathrm{PES}}$	δ	$\tilde{\nu}_{\mathrm{exp}}$	
632-633	3	$4_1 + 10_1$	E	3651.4			
634-635	3,4	$[5_1 + 7_1, 5_1 + 11_1]$	E	3653.8			
636	3	$10_1 + 5_1, 4_1 + 5_1$	A_2	3654.2			
637	3	$10_1 + 5_1, 4_1 + 5_1$	A_1	3654.6			
638-639	0	$4_1 + 11_1 + 8_1, 10_1 + 7_1 + 8_1$	E	3657.5			
640-641	0,2	$[11_1 + 7_1 + 8_1, 6_3]$	E	3660.9			
642-643	0	$[5_1 + 11_1 + 7_1, 5_1 + 11_2]$	E	3665.4			
644	1	$[11_1 + 7_2, 11_3]$	A_2	3665.6			
645-646	3	5_2	E	3672.9			
647	0	6_3	A_1	3673.2			
648	0,1	$[5_1 + 11_1 + 7_1, 5_1 + 11_1 + 7_1]$	A_2	3673.7			
649-650	0	$[6_2 + 8_1, 6_2 + 8_1]$	E	3678.5			
651-652	3,4	$5_1 + 7_1, 5_1 + 11_1$	E	3682.2			
653-654	5,6	$[4_1, 10_1]$	E	3682.3			
655-656	3	$[4_1 + 5_1, 10_1 + 5_1]$	E	3682.7			
657	3	$[10_1 + 7_1, 4_1 + 11_1]$	A_1	3684.8			
658	3	$4_1 + 7_1, 10_1 + 11_1$	A_2	3685.0			
659	4	$10_1 + 11_1, 4_1 + 7_1$	A_1	3685.3			
660	0	1_1	A_1	3686.4	[−1.1]	3685.3	10
661	0,4	$[10_1 + 11_1 + 7_1, 10_1 + 7_1]$	A_2	3687.5			
662-663	0,2	$[7_3, 11_3]$	E	3688.2			
664	3	$[2_1, 9_1]$	A_2	3688.6			
665	3	$[2_1, 9_1]$	A_1	3688.7			
666-667	0	$[4_1 + 11_1 + 7_1, 4_1 + 6_1 + 7_1]$	E	3689.9			
668-669	0	1_1	E	3692.6	[−1.0]	3691.6	10
670	5	5_1	A_2	3692.7			
671	6	5_1	A_1	3692.8			
672-673	4	$6_1 + 8_1$	E	3695.1			
674	4	$[4_1 + 7_1, 10_1 + 11_1]$	E	3696.4			
675	4	$[10_1 + 7_1, 4_1 + 11_1]$	A_2	3696.7			

[1] A. Sunaga, T. Győri, G. Czakó, and E. Mátyus, Exact quantum dynamics of methanol: Full-dimensional ab initio potential energy surface of spectroscopic quality and variational vibrational states, J. Chem. Phys. **163**, 064101 (2025).

[2] I. Batatia, D. P. Kovacs, G. Simm, C. Ortner, and G. Csanyi, MACE: Higher order equivariant message passing neural networks for fast and accurate force fields, in *Advances in Neural Information Processing Systems*, Vol. 35, edited by S. Koyejo, S. Mohamed, A. Agarwal, D. Belgrave, K. Cho, and A. Oh (Curran Associates, Inc., 2022) pp. 11423–11436.

[3] A. Sunaga, G. Avila, and E. Mátyus, Variational vibrational states of methanol (12D), J. Chem. Theory Comput. **20**, 8100 (2024).

[4] D. F. Dinu, K. Oenen, J. Schlagin, M. Podewitz, H. Grothe, T. Loerting, and K. R. Liedl, How vibrational notations can spoil infrared spectroscopy: A case study on isolated methanol, ACS Phys. Chem. Au **4**, 679 (2024).

[5] X. Wang and D. S. Perry, An internal coordinate model of coupling between the torsion and C–H vibrations in methanol, J. Chem. Phys. **109**, 10795 (1998).

[6] T. N. Clasp and D. S. Perry, Torsion-vibration coupling in methanol: the adiabatic approximation and intramolecular vibrational redistribution scaling, J. Chem. Phys. **125**, 104313 (2006).

[7] A. Serrallach, R. Meyer, and H. Günthard, Methanol and deuterated species: Infrared data, valence force field, rotamers, and conformation, J. Mol. Spectrosc. **52**, 94 (1974).

[8] V. Hänninen, M. Horn, and L. Halonen, Torsional motion and vibrational overtone spectroscopy of methanol, J. Chem. Phys. **111**, 3018 (1999).

[9] L. H. Xu, X. Wang, T. J. Cronin, D. S. Perry, G. T. Fraser, and A. S. Pine, Sub-Doppler infrared spectra and torsion-rotation energy manifold of methanol in the CH-stretch fundamental region, J. Mol. Spectrosc. **185**, 158 (1997).

[10] R. H. Hunt, W. N. Shelton, F. A. Flaherty, and W. B. Cook, Torsion-rotation energy levels and the hindering potential barrier for the excited vibrational state of the OH-stretch fundamental band nu1 of methanol, J. Mol. Spectrosc. **192**, 277 (1998).